Automatic Cardiac Rhythm Classification With Concurrent Manual Chest Compressions

**IRAIA ISASI[1], UNAI IRUSTA[1], (Member, IEEE), ALI BAHRAMI RAD[2], (Member, IEEE),
ELISABETE ARAMENDI[1], (Member, IEEE), MORTEZA ZABIHI[3], (Student Member, IEEE),
TRYGVE EFTESTØL[4], (Senior Member, IEEE), JO KRAMER-JOHANSEN[5], AND LARS WIK[5]**

[1]Department of Communications Engineering, University of the Basque Country UPV/EHU, 48013 Bilbao, Spain
[2]Department of Electrical Engineering and Automation, Aalto University, 02150 Espoo, Finland
[3]Department of Computing Sciences, Tampere University, 33720 Tampere, Finland
[4]Department of Electrical Engineering and Computer Science, University of Stavanger, 4036 Stavanger, Norway
[5]Norwegian National Advisory Unit on Prehospital Emergency Medicine (NAKOS), Oslo University Hospital and University of Oslo, 0424 Oslo, Norway

Corresponding author: Iraia Isasi (iraia.isasi@ehu.eus)

ABSTRACT Electrocardiogram (EKG) based classification of out-of-hospital cardiac arrest (OHCA) rhythms is important to guide treatment and to retrospectively elucidate the effects of therapy on patient response. OHCA rhythms are grouped into five categories: ventricular fibrillation (VF) and tachycardia (VT), asystole (AS), pulseless electrical activity (PEA), and pulse-generating rhythms (PR). Clinically these rhythms are grouped into broader categories like shockable (VF/VT), non-shockable (AS/PEA/PR), or organized (ORG, PEA/PR). OHCA rhythm classification is further complicated because EKGs are corrupted by cardiopulmonary resuscitation (CPR) artifacts. The objective of this study was to demonstrate a framework for automatic multiclass OHCA rhythm classification in the presence of CPR artifacts. In total, 2133 EKG segments from 272 OHCA patients were used: 580 AS, 94 PR, 953 PEA, 479 VF, and 27 VT. CPR artifacts were adaptively filtered, 93 features were computed from the stationary wavelet transform analysis, and random forests were used for classification. A repeated stratified nested cross-validation procedure was used for feature selection, parameter tuning, and model assessment. Data were partitioned patient-wise. The classifiers were evaluated using per class sensitivity, and the unweighted mean of sensitivities (UMS) as a global performance metric. Four levels of clinical detail were studied: shock/no-shock, shock/AS/ORG, VF/VT/AS/ORG, and VF/VT/AS/PEA/PR. The median UMS (interdecile range) for the 2, 3, 4, and 5-class classifiers were: 95.4% (95.1-95.6), 87.6% (87.3-88.1), 80.6% (79.3-81.8), and 71.9% (69.5-74.6), respectively. For shock/no-shock decisions sensitivities were 93.5% (93.0-93.9) and 97.2% (97.0-97.4), meeting clinical standards for artifact-free EKG. The UMS for five classes with CPR artifacts was 5.8-points below that of the best algorithms without CPR artifacts, but improved the UMS of latter by over 19-points for EKG with CPR artifacts. A robust and accurate approach for multiclass OHCA rhythm classification during CPR has been demonstrated, improving the accuracy of the current state-of-the-art methods.

INDEX TERMS Out-of-hospital cardiac arrest (OHCA), electrocardiogram (EKG), cardiopulmonary resuscitation (CPR), adaptive filter, stationary wavelet transform (SWT), random forest (RF) classifier.

I. INTRODUCTION

Out-of-hospital cardiac arrest (OHCA) is a leading cause of death in the industrialized world. In Europe the estimated annual average incidence of ambulance treated cases is 41 (range 19-104) per 100 000 persons [1]. Patients in cardiac arrest lose their cardiac and respiratory function, and die within minutes if not treated. Treatment consists of highly time-sensitive interventions such as: recognition, call for help, cardiopulmonary resuscitation (CPR), defibrillation, and post-resuscitation care. Bystanders and lay rescuers can provide CPR to maintain an artificial perfusion of the vital

The associate editor coordinating the review of this manuscript and approving it for publication was Nuno Garcia.

organs through chest compressions, and mouth to mouth breaths for ventilations. Defibrillation by an automated external defibrillator (AED) can be used to revert lethal ventricular arrhythmia and restore the normal function of the heart. Upon the arrival of the medicalized ambulance, specialized treatment becomes available including continued high-quality CPR and defibrillation, but also add intravenous pharmacological treatment (adrenaline and anti-arrhythmic drugs), airway management, and assisted ventilation. If spontaneous circulation is restored, the patient is transported to a hospital for in-hospital treatment and post-resuscitation care [2].

Knowing the patient's cardiac rhythm during resuscitation is important for two reasons. First, awareness of the patient's rhythm may contribute to guide therapy. International guidelines describe treatment pathways based on cardiac rhythm and elapsed time, i.e., rhythm analysis every 2 minutes with defibrillation attempts for ventricular fibrillation (VF) or tachycardia (VT), and consideration of intravenous drugs such as adrenaline every 3-5 minutes for all non-perfusing rhythms [2]. Second, in retrospective analyses, the rhythm transitions of the patient during CPR provide important information about the interplay between therapy and patient response [3]–[5]. This may contribute to identify therapeutic interventions or treatment patterns that improve OHCA survival. One of the limiting factors for such analyses is the lack of datasets with cardiac rhythm annotations due to the manual labor involved. Thus, there is a need for automatic methods for cardiac rhythm annotation. In OHCA rhythms are grouped into five categories [6], [7]: VF, VT, asystole (AS), pulseless electrical activity (PEA), and pulse-generating rhythms (PR). Often, PEA and PR are called organized rhythms (ORG), or rhythms presenting visible QRS complexes in the electrocardiogram (EKG) [8]. PEA is characterized by a disassociation between the mechanical (contraction of the myocardium) and electrical (QRS complexes) activities of the heart, which leads to no palpable pulse [4].

OHCA rhythm classification algorithms are based on the analysis of the EKG, and in most cases address 2-class classification problems. A typical example is AED shock advice algorithms [9]–[11], designed to discriminate shockable (VF/VT) from nonshockable rhythms (AS/ORG). Depending on the clinical context a finer detail is needed. VT treatment may benefit from synchronized electrical cardioversion [12]. Another clinically relevant problem is the detection of spontaneous circulation or pulse, which is framed as a PEA/PR discrimination algorithm once ORG rhythms are identified [8], [13], [14]. So there is clearly a need for different levels of detail in OHCA cardiac rhythm classification. Five-class OHCA rhythm classification using the EKG was introduced by Rad *et al.*, [7], [15] using features obtained from the discrete wavelet transform (DWT) sub-band decomposition of an artifact-free EKG. Most OHCA rhythm classification algorithms consist of an EKG feature extraction stage followed by a machine learning classifier. EKG feature extraction has been approached in the time [16], [17], frequency [18], [19], time-frequency [15], [20], [21],

and complexity domains [22], [23]. The machine learning approaches explored in the classification stage include K-nearest neighbors [15], [24], support vector machines [10], [25], [26], artificial neural networks [13], [19], [27], and ensembles of decision trees [11], [14].

OHCA rhythm classification is further complicated by the presence of CPR artifacts in the EKG. Interruptions in CPR to classify the rhythm lead to interrupted perfusion of vital organs and lowers chances of survival [28]. Efforts have been made to develop accurate OHCA rhythm analysis methods during CPR [29]. The most popular approach is the suppression of the CPR artifact using adaptive filters [30]–[32], followed by an EKG feature extraction stage on the filtered EKG. These approaches have been successfully demonstrated to discriminate shockable (Sh) from nonshockable (NSh) rhythms both during manual CPR [33] and piston driven mechanical CPR [21]. In fact, an improved feature extraction based on the stationary wavelet transform (SWT) sub-band decomposition has yielded improved classification results for shock/no-shock decisions during mechanical CPR, and is the basis for feature extraction in this work. However, there are no studies on multiclass OHCA rhythm classification during CPR. In fact, when 5-class OHCA rhythm classifiers developed using artifact-free EKG were tested during CPR their performance substantially degraded [15], [27]. So there is a need to develop algorithms for multiclass OHCA rhythm classification during CPR.

This study introduces new methods for multiclass OHCA rhythm classification during CPR, using features obtained from the SWT analysis of the EKG after filtering CPR artifacts. The scope of the algorithms is gradually increased from 2-class to 5-class rhythm classification to address the different levels of clinical detail needed depending on the application. The following classification problems were studied: Sh/NSh, Sh/AS/ORG, VF/VT/AS/ORG, and VF/VT/AS/PEA/PR. The paper is organized as follows. The study dataset and its annotation are described in Section II; feature engineering including CPR artifact filtering is described in Section III; Section IV describes the architecture used for the optimization and evaluation of the classification algorithms. Finally, results, discussion, and conclusions are presented in Sections V-VII.

II. DATA COLLECTION AND PREPARATION

Data were extracted from a large prospective OHCA clinical trial designed to measure CPR-quality, and conducted in three European sites between 2002 and 2004: Akershus (Norway), Stockholm (Sweden) and London (UK) [34], [35]. Prototype defibrillators based on the Heartstart 4000 (Philips Medical Systems, Andover, Mass) were deployed in 6 ambulances at each site. The defibrillators were fitted with an external CPR assist pad that measured compression depth [36]. The raw data for our study consisted of the EKG and transthoracic impedance obtained from the defibrillation pads, and the compression depth. All signals were originally sampled at 500 Hz, and then downsampled to a sampling frequency of
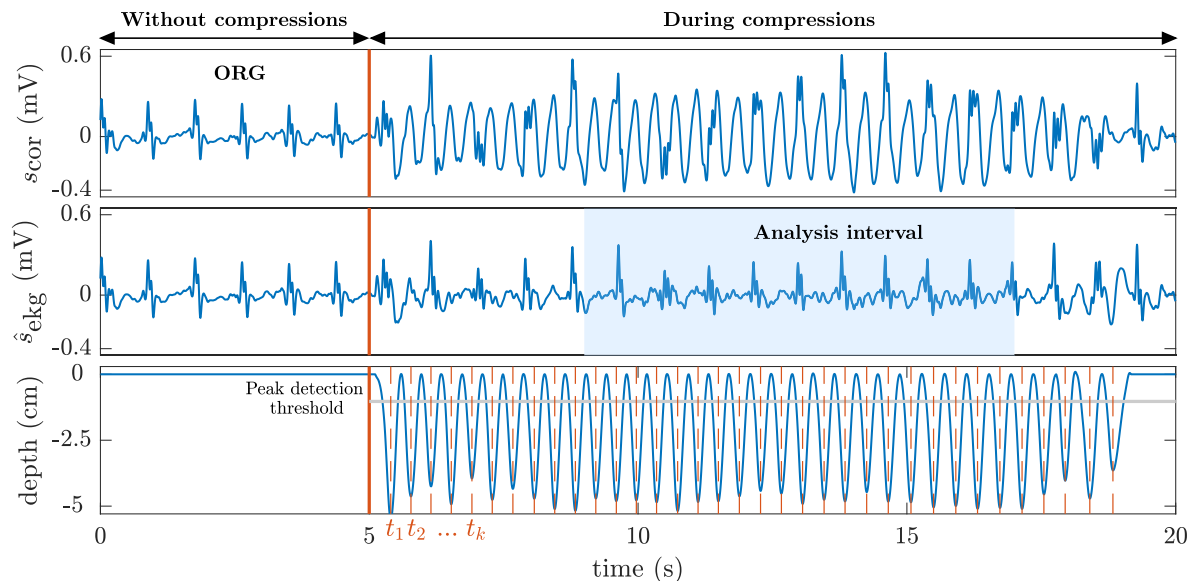
FIGURE 1. One 20-s segment from the dataset corresponding to a patient with an organized rhythm (ORG). In the first 5 s there is no artifact and the ORG rhythm is visible, in the last 15 s the CPR artifact conceals the patient's rhythm. After filtering $\hat{s}_{ekg}$ is obtained (middle panel), and the underlying rhythm is again visible in the artifacted interval. The bottom panel shows the compression depth signal with the chest compression instants (t_k) highlighted using vertical red lines.

$f_s = 250\,Hz\,(T_s = 4\,\text{ms})$ for this study. A notch and a Hampel filter were used to remove powerline interferences and spiky artifacts, respectively. Chest compression instants (t_k), were automatically marked in the depth signal using a negative peak detector for depths exceeding 1 cm (see Fig. 1).

All recordings were annotated for the original study into the five OHCA rhythm types, by consensus between an experienced anesthesiologist trained in advanced cardiac life support and a biomedical engineer specialized in resuscitation [34]. VF was defined as an irregular ventricular rhythm with peak-to-peak amplitudes above $100\,\mu V$ and a fibrillation frequency above 2 Hz. Regular ventricular rhythms with rates above $120\,\text{min}^{-1}$ were annotated as VT. AS was annotated in rhythms with peak-to-peak amplitude below $100\,\mu V$ and/or rates below $12\,\text{min}^{-1}$, and ORG rhythms when the heart rate was above 12 min^{-1}. ORG rhythms were further classified into PEA or PR by assessing the presence of blood flow, indicated by clinical annotations of pulse done during resuscitation, or by the presence of fluctuations in the thoracic impedance aligned with the QRS complexes [13], [34].

For this study, we automatically extracted 20-s segments with the following characteristics: unique rhythm type, ongoing compressions during a 15-s interval, and a 5-s interval without compressions either preceding or following chest compressions (see Fig. 1). The interval during compressions was used to develop and evaluate the OHCA rhythm classifiers, and the interval without compression artifacts to confirm the original rhythm annotation. All automatically extracted segments were reviewed by 3 experienced biomedical engineers to discard segments with low signal quality and noise, and to certify by consensus that the original annotations in the dataset were correct. The final dataset contained

2133 segments from 272 patients, whereof 580 were AS (139 patients), 94 PR (31), 953 PEA (167), 479 VF (103), and 27 VT (11).

III. FEATURE ENGINEERING

Feature engineering consisted of 3 stages. First, chest compression artifacts were removed using an adaptive filter. Then, a multi-resolution analysis of the EKG was performed using wavelet transforms, from which the denoised EKG and its sub-band decomposition were obtained. Finally, high-resolution features were extracted from the denoised EKG and its sub-band components. In what follows n is the sample index, so $t = n \cdot T_s$.

A. CPR ARTIFACT FILTER

CPR artifacts were suppressed using a state-of-the-art method based on a recursive least squares (RLS) filter [32] that estimates the CPR artifact, $s_{cpr}(n)$, as a quasiperiodic interference [31]. The fundamental frequency of the artifact, $\omega_0(n)$, is the instantaneous frequency of the chest compressions. The CPR artifact is represented as a truncated Fourier series of N harmonically related components of frequencies $\omega_\ell = \ell \cdot \omega_0$ and slowly time-varying Fourier coefficients [31]:

$$s_{cpr}(n) = A(n)\sum_{\ell=1}^{N} a_\ell(n)\cos(\omega_\ell n) + b_\ell(n)\sin(\omega_\ell n)$$
$$= A(n)\mathbf{\Theta}^{\mathsf{T}}(n)\mathbf{\Phi}(n) \tag{1}$$

where

$$\mathbf{\Phi}(n = [\cos(\omega_1 n)\ \sin(\omega_1 n)\ldots\cos(\omega_N n)\ \sin(\omega_N n)]^{\mathsf{T}} \tag{2}$$
$$\mathbf{\Theta}(n) = [a_1(n)\,b_1(n)\ \ldots\ a_N(n)\,b_N(n)]^{\mathsf{T}} \tag{3}$$

and $A(n) = 1$ during compressions, and $A(n) = 0$ otherwise. The time-varying coefficients of the RLS filter are the in-phase (a_ℓ) and quadrature (b_ℓ) components in vector $\mathbf{\Theta}(n)$. The instantaneous frequency of the compressions was derived from the t_k instants obtained from the depth signal (see Fig. 1):

$$\omega_0(n) = 2\pi \frac{1}{t_k - t_{k-1}} \qquad t_{k-1} \le nT_s < t_k \qquad (4)$$

The RLS coefficients were adaptively estimated to minimize the mean square error between the corrupted EKG, s_{cor}, and the estimated artifact, $\hat{s}_{\text{cpr}}$, at the frequency of the harmonics. The error signal of the RLS filter is thus the filtered EKG, $\hat{s}_{\text{ekg}}$, which is used to identify the underlying rhythm. The RLS update equations are [37]:

$$\hat{s}_{\text{ekg}}(n) = s_{\text{cor}}(n) - A(n)\mathbf{\Theta}^{\mathsf{T}}(n-1)\mathbf{\Phi}(n) \qquad (5)$$

$$\mathbf{F}(n) = \frac{1}{\lambda}\left[\mathbf{F}(n-1) - \frac{\mathbf{F}(n-1)\mathbf{\Phi}(n)\mathbf{\Phi}^{\mathsf{T}}(n)\mathbf{F}(n-1)}{\lambda + \mathbf{\Phi}^{\mathsf{T}}(n)\mathbf{F}(n-1)\mathbf{\Phi}(n)}\right] \qquad (6)$$

$$\mathbf{\Theta}(n) = \mathbf{\Theta}(n-1) + \mathbf{F}(n)\mathbf{\Phi}(n)\hat{s}_{\text{ekg}}(n) \qquad (7)$$

The gain matrix and coefficients vector were initialized to $F(0) = 0.03 \cdot \mathbf{I}_{2N}$ and $\Theta(0) = \mathbf{0}$, where $\mathbf{I}_{2N}$ is the $2N \times 2N$ identity matrix. The forgetting factor of the RLS algorithm, λ, and the number of harmonics, N, were set to 0.998 and 4, as recommended in [32].

B. STATIONARY WAVELET TRANSFORM

EKG multiresolution analysis was done using the SWT, which differs from the standard DWT in that at each decomposition level the low-pass (approximation) and high-pass (detail) components are not downsampled. Instead, the filters are upsampled so all detail and approximation coefficients have the length of the original signal, producing a translation-invariant representation [38].

Each EKG segment was decomposed into its sub-bands using a pair of quadrature mirror lowpass (h_j) and highpass (g_j) filters, which for level 0 are related by:

$$g_0(L - 1 - n) = (-1)^n h_0(n), \qquad (8)$$

where L is the length of the filters. At stage j the filters were those of stage 0 upsampled by a 2^j factor, $h_j(n) = h_0(n)_{\uparrow 2^j}$. The detail, $d_j(n)$, and approximation, $a_j(n)$, coefficients were recursively obtained through convolution ($*$):

$$a_0(n) = \hat{s}_{\text{ekg}}(n) \qquad (9)$$

$$a_j(n) = h_{j-1}(n) * a_{j-1}(n) \qquad (10)$$

$$d_j(n) = g_{j-1}(n) * a_{j-1}(n) \qquad (11)$$

The time-reversed version of the decomposition filters, that is $\overline{h}(n) = h(L - 1 - n)$, were recursively used to reconstruct the original signal [38]:

$$a_{j-1}(n) = \tfrac{1}{2}\left(\overline{h_j}(n) * a_j(n) + \overline{g_j}(n) * d_j(n)\right) \qquad (12)$$

from $j = J, \ldots, 1$.

EKG features were extracted using a 2048-sample analysis interval (8.192 s) of $\hat{s}_{\text{ekg}}$ centered in the 15 s during chest

compressions (see Fig. 1). A Daubechies 4 mother wavelet and $J = 7$ decomposition levels were used to generate a_7 and $d_7, \ldots, d_1$. Only detail coefficients $d_3 - d_7$ were used for feature extraction, which is equivalent to retaining the spectral components in the $0.98 - 31.25\,Hz$ band. Soft denoising was applied to $d_3 - d_7$ with a universal threshold rescaled by the standard deviation of the noise [39]. The denoised $d_3 - d_7$ coefficients were used to obtain the denoised EKG, $\hat{s}_{\text{den}}$, by recursively applying eq. (12). The whole decomposition and denoising (reconstruction) processes are illustrated in Fig. 2 for two rhythms, a VF and an ORG.

C. FEATURE EXTRACTION

Ninety three features were extracted from $\hat{s}_{\text{den}}$ and $d_3 - d_7$. These features quantify the most distinctive characteristics of OHCA rhythm subtypes, and encompass the collective knowledge of over 25 years of active research in the field (over 250 features from the available literature were initially analyzed). In what follows, feature naming is that of the original papers, and the MATLAB code for feature calculation is available from (https://github.com/iraiaisasi/OHCAfeatures). The features grouped by analysis domain are:

- *Time domain* (5 features). These were only extracted from $\hat{s}_{\text{den}}$ and include: bCP [18], x1, x2 [33], and the mean and the standard deviation of the heart rate (MeanRate and StdRate) obtained from the QRS detections of a modified Hamilton-Tompkins algorithm [14], [40].
- *Spectral domain* (6 features). Including the classical x3, x4, x5 [33], VFleak [41], and two new features, Enrg, the relative energy content of the signal in the 4-8 Hz frequency band, and SkewPSD, the skewness of the power spectral density of the EKG. All features were computed from $\hat{s}_{\text{den}}$.
- *Complexity analysis* (14 features), including CVbin and Abin [42] of $\hat{s}_{\text{den}}$, and two measures of entropy for $\hat{s}_{\text{den}}$ and $d_3 - d_7$. The entropy measures were the sample entropy (SampEn) of the signal, and the Shannon entropy (ShanEn) of the sign of the first difference [43].
- *Statistical analysis* (54 features). Nine features were calculated to characterize the statistical distribution of the signal amplitude: interquartile ranges (IQR) [15], mean and standard deviation of the absolute value of the amplitudes (MeanAbs and StdAbs) and slopes (MeanAbs1 and StdAbs1), Skewness (Skew), Kurtosis (Kurt) [11], and the Hjorth mobility and complexity (Hmb and Hcmp) [44]. All the features were computed for $\hat{s}_{\text{den}}$ and $d_3 - d_7$.
- *Phase space features* (14 features). Taken's time-delay embedding method [45] with a delay of $\tau = 2$ samples was used to create a two-dimensional phase space representation for $\hat{s}_{\text{den}}$ and $d_3 - d_7$ [46]. An ellipsoid was fitted in the phase-space using the least squares criterion, and its major axis (EllipPS), and the skewness of
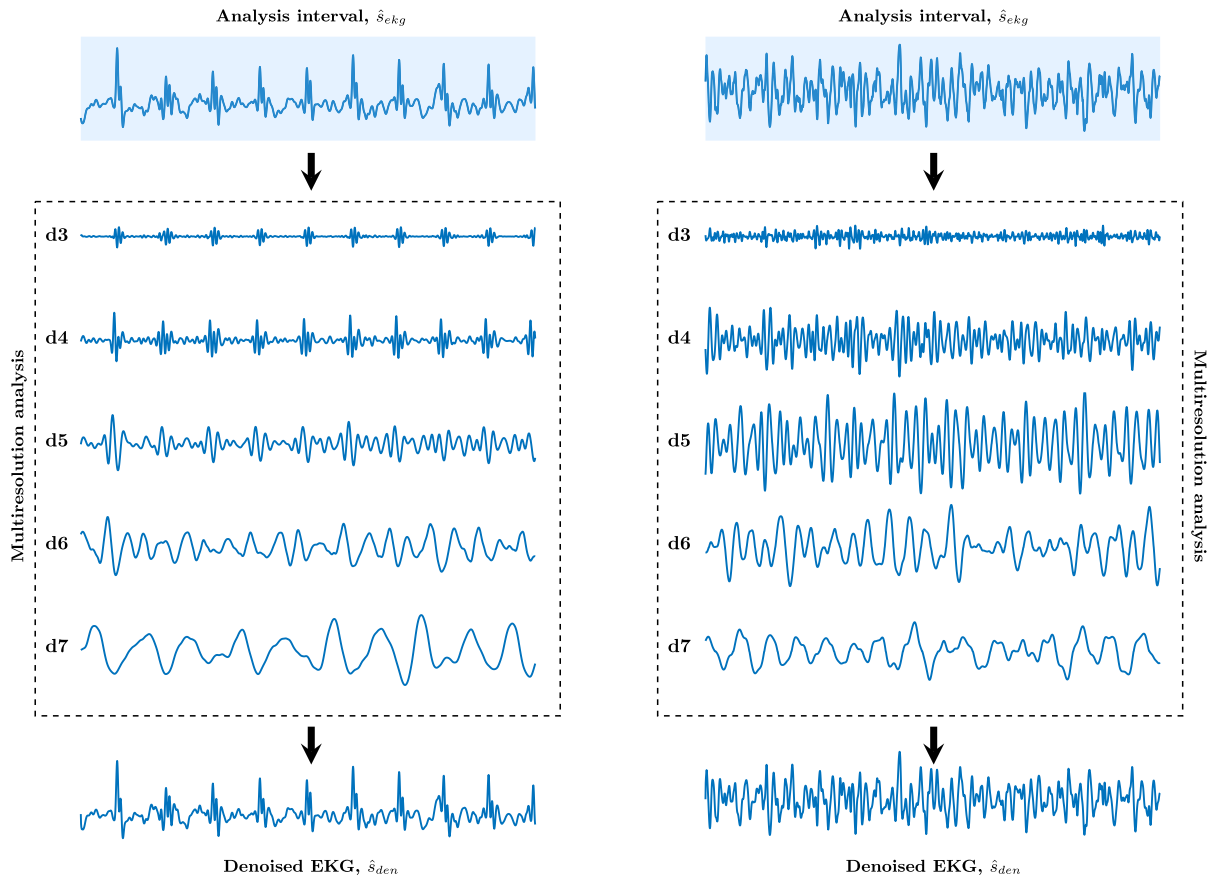
FIGURE 2. SWT sub-band decomposition and denoised EKG reconstruction for the 8.192-s analysis interval of the filtered EKG, $\hat{s}_{ekg}$. The left panel corresponds to an organized rhythm (ORG) and the right panel to a ventricular fibrillation (VF).

the distance distributions in the phase space (SkewPS) were computed. Then a recurrence quantification analysis (RQA) was used to extract and quantify the transition structures of the system dynamics in the phase space. Two RQA measures were computed only for $\hat{s}_{den}$, the length of the longest diagonal line (RQA1), and the recurrence period density entropy (RQA2) [47].

The dataset can thus be represented as a set of instance-label pairs $\{(x_1, y_1), ..., (x_N, y_N)\}$ where y_i are the class labels (for instance $\{0, 1\}$ for a Sh/NSh classification problem), the feature vector $x_i \in \mathbb{R}^K$ contains the values of the $K = 93$ features for EKG segment i, and $N = 2133$ is the number of EKG segments in the database.

IV. CLASSIFIER TRAINING AND EVALUATION

A repeated quasi-stratified nested cross-validation (CV) architecture was used [21], [48], with an outer 10-fold CV for feature selection and model assessment, and an inner 5-fold CV for classifier parameter optimization. First, for each training set of the outer CV, features were selected using recursive feature elimination (RFE) [49]. Then, these features were used in the inner CV to optimize the parameters of the classifier. Finally, the classifier was trained and assessed in the outer loop. Data were always partitioned patient-wise

and in a quasi-stratified manner, by forcing the prevalence of each rhythm in each fold to be at least 70% of the prevalence of that rhythm in the whole set. In this way patient-wise and stratified sampling could be done simultaneously.

Confusion matrices were used to evaluate the performance of the classifiers [15], and four classification problems were addressed: Sh/NSh (2-class), Sh/AS/ORG (3-class), VF/VT/AS/ORG (4-class), and VF/VT/AS/PEA/PR (5-class). For each class i the sensitivity (Se_i) was computed, and the unweighted mean of all sensitivities (UMS) was used as summarizing metric:

$$Se_i = \frac{TP_i}{TP_i + FN_i}, \quad UMS = \frac{1}{P}\sum_{i=1}^{P} Se_i \quad (13)$$

where TP_i and FN_i are the true positives and false negatives for class i, and P is the number of classes. The nested CV procedure was repeated 50 times to estimate the statistical distributions of Se_i and UMS, and to obtain the stacked confusion matrices for each classification problem.

A. CLASSIFIER

Random forest (RF) classifiers [50] were used to decide the EKG rhythm class. An RF is an ensemble of B decision
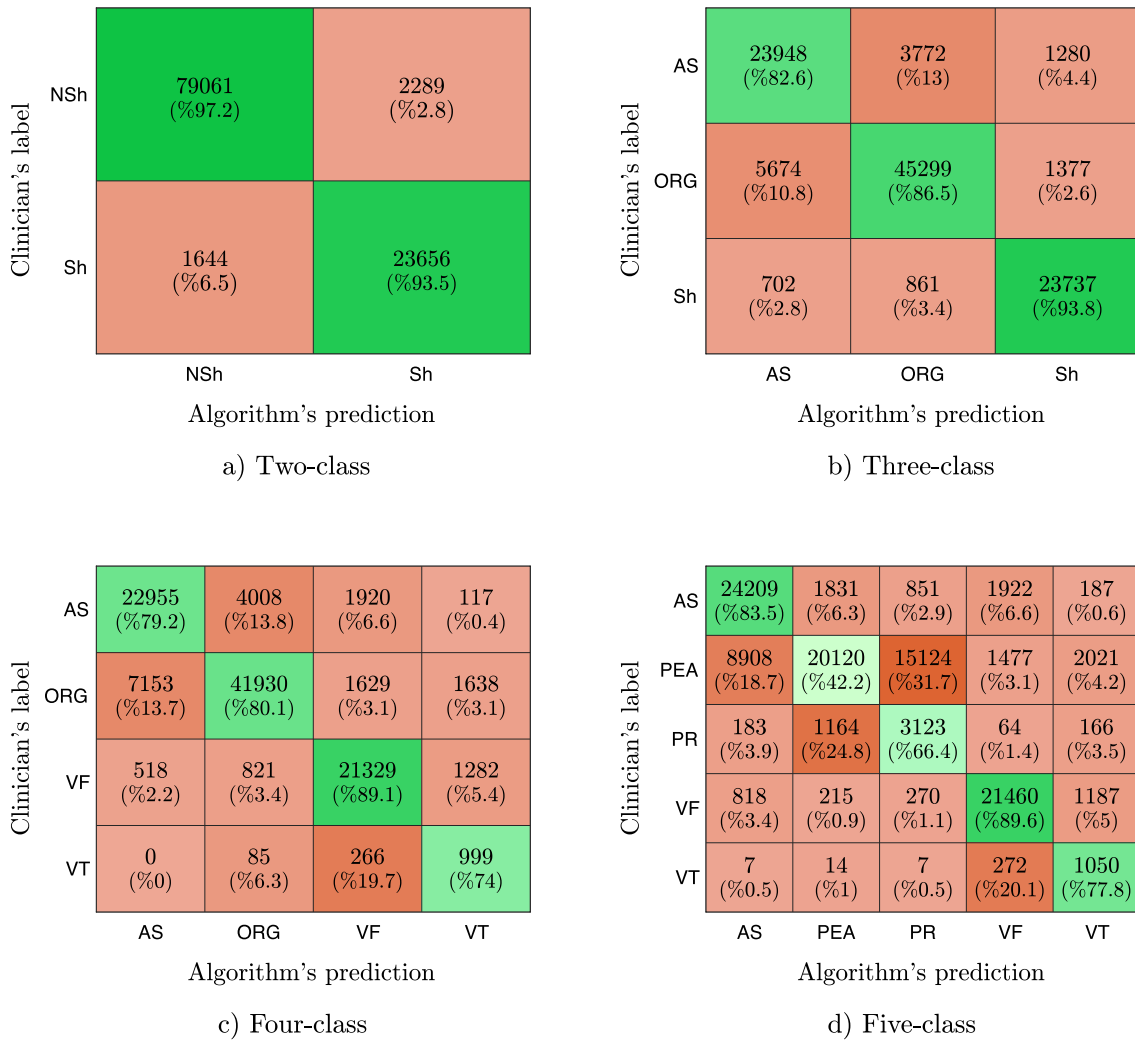
FIGURE 3. Stacked confusion matrices for 50 runs of the nested CV procedure for the different models. The mean sensitivities for each class and model are shown in the diagonals (mean and median sensitivities are slightly different, see table 1).

trees $\{T_1(\boldsymbol{x}), ..., T_B(\boldsymbol{x})\}$ that produces B nearly uncorrelated predictions $\{\hat{y}_1 = T_1(\boldsymbol{x}), ..., \hat{y}_B = T_B(\boldsymbol{x})\}$ of the rhythm type for the EKG segment. Training an RF classifier comprises:

- Generating B training subsets from the original training data by bootstrapping (i.e., random sampling with replacement). We choose each training subset to have the same size as the original training data.
- A classification tree is grown for each training subset by choosing the best split among a randomly selected subset of m_{try} features in each node. The criterion to choose the split was to minimize the cross-entropy.
- The recursive binary splitting continues until each terminal node has fewer than some minimum number of observations, l_{size}.
- The decision of classifier, $\hat{y}_j = F_{RF}(\boldsymbol{x}_j)$, is obtained by the majority vote of the B trees.

Once the models were trained, the predictions in the validation sets were obtained by comparing the predictions of the model $\hat{y}_j$ to the labels assigned by the clinicians y_j, to obtain the confusion matrix of the model and the metrics derived thereof.

We considered three parameters of the RF classifier: B, m_{try}, and l_{size}. The number of trees was initially fixed to $B = 500$. This choice is not critical, a sufficiently large number stabilizes the accuracy and further increasing B does not overfit the model [50]. The number of predictors per split was set to the default value $\sqrt{K}$. The minimum number of observations per leaf, l_{size}, controls the depth of the trees, and was identified as critical in our preliminary tests. We optimized l_{size} in the inner CV by doing a grid-search in the range $1 \leq l_{size} \leq 200$ with the UMS as the objective function. Finally, uniform prior probabilities for each class were assigned during training to address the class imbalance.

B. FEATURE SELECTION

Feature selection was based on an RFE approach using the permutation importance as a ranking criterion [51]–[53]. Permutation importance is a built-in characteristic of the RF
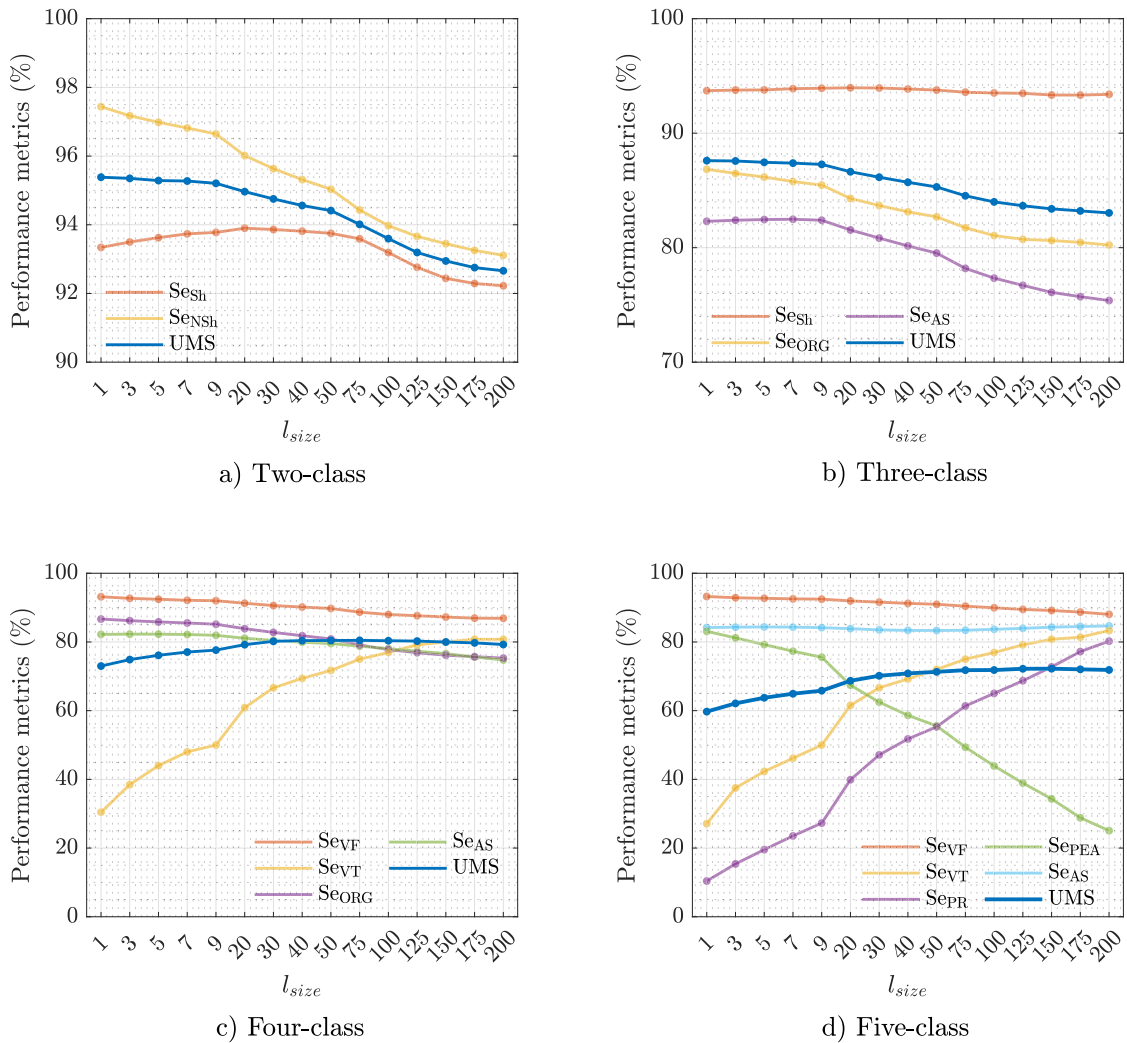
a) Two-class

b) Three-class

c) Four-class

d) Five-class

FIGURE 4. Median UMS and Se per class in the 50 repeats of the 10-fold outer CV, as a function of l_{size}.

classifier that ranks feature importance by permuting the values of the feature in the training data and assessing the out-of-bag error. Large errors mean the feature is important for classification. At each iteration of the RFE algorithm, features were ranked and the least important 3% of the features were removed. The process was continued until K_{cl} features were left for classification. The values decided for the different models were: $K_{cl} = 25$ for 2-class, $K_{cl} = 30$ for 3-class, $K_{cl} = 35$ for 4-class, and $K_{cl} = 40$ for 5-class.

V. RESULTS
The results reported in this section are those obtained after running the RFE feature selection algorithm in the 10-fold outer CV until K_{cl} features were left, and fitting the classifiers with the optimal parameters determined in the 5-fold inner CV. The process was repeated in 50 random repetitions of the nested CV procedure, there are thus 50 estimates of the metrics for the whole dataset and 500 algorithmic runs on the validation folds in the outer CV. The metrics are reported as median (interdecile range, IDR) for those 50 evaluations.

A detailed analysis of the classification results for the different class models are shown in Table 1 and Fig. 3. Fig. 3 shows the confusion matrices obtained stacking the predictions from the 50 random repetitions of the nested CV procedure, and provide all the information needed to accurately calculate the performance metrics for each rhythm type and classifier. The median (IDR) of the sensitivities and UMS for each classifier are shown in Table 1. The clinical relevance of the classification results and classification errors is addressed in section VI, the discussion.

As reference, we also computed the classification results when the features were selected exclusively on the feature's permutation importance. That is, the RFE algorithm was substituted by a single feature ranking based on importance from which the K_{cl} most important features were selected. Using a single feature ranking based on importance the median (IDR) UMS for the 2, 3, 4 and 5-class classifiers were 95.3% (95.0-95.5), 87.3% (86.9-87.6), 81.1% (79.5-82.3), and 67.8% (65.7-70.0), respectively. The classification results for 2, 3, and 4 classes were similar to those obtained using

TABLE 1. Median UMS and sensitivity per class for different classifiers. The metrics are reported as median (IDR) for the 50 runs of the nested CV procedure.

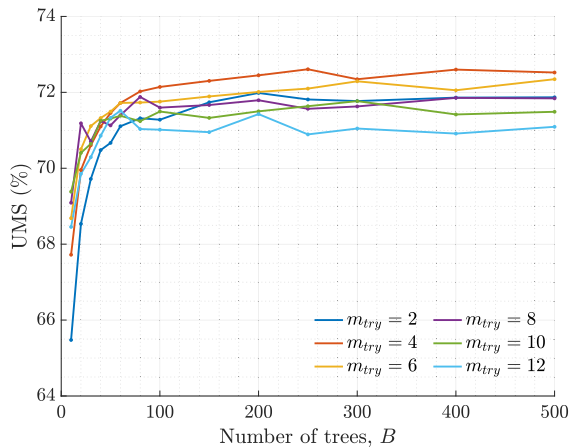| Classifier	Se (%)	UMS (%)
Two-class		
Sh	93.5 (93.0-93.9)	**95.4 (95.1-95.6)**
NSh	97.2 (97.0-97.4)	
Three-class		
AS	82.5 (81.6-83.4)	
OR	86.5 (86.0-87.1)	**87.6 (87.3-88.1)**
Sh	93.9 (93.3-94.3)	
Four-class		
AS	79.0 (78.1-80.3)	
OR	80.1 (78.8-81.3)	**80.6 (79.3-81.8)**
VF	89.1 (88.2-89.8)	
VT	74.1 (70.4-77.8)	
Five-class		
AS	83.4 (81.9-85.1)	
PEA	42.6 (37.6-46.9)	
PR	65.4 (60.1-73.9)	**71.9 (69.5-74.6)**
VF	89.6 (88.5-90.6)	
VT	77.8 (66.7-88.9)	

FIGURE 5. The median UMS (5-class) in the 50 random repetitions, as a function of the number of trees, *B*, and the number of features per split, m_{try}.

RFE feature selection, but an advanced feature selection approach combining feature importance and sequential feature elimination boosted the 5-class classification results by 4-points.

A. SELECTION OF PARAMETERS

The most critical parameter in our RF classifiers was the minimum number of observations in the terminal nodes, l_{size}, which gives a compromise between bias and variance by controlling how shallow the classification trees are. Larger values of l_{size} produce shallower trees. Fig. 4 shows, for the different classifiers, the median value of the performance metrics for the evaluations of the 50 repeats of the 10-fold outer CV as a function of l_{size}. In the cases where class imbalance is smaller (2 and 3 class) deeper trees increase the UMS, however when the class imbalance is large (4 and 5 class) shallower trees produce better results (see Fig. 4). The median (IDR) value of the optimal l_{size} for the 2 and 3-class classifiers were 3 (1.0-7.0) and 3 (1.0-5.0), but increased considerably to
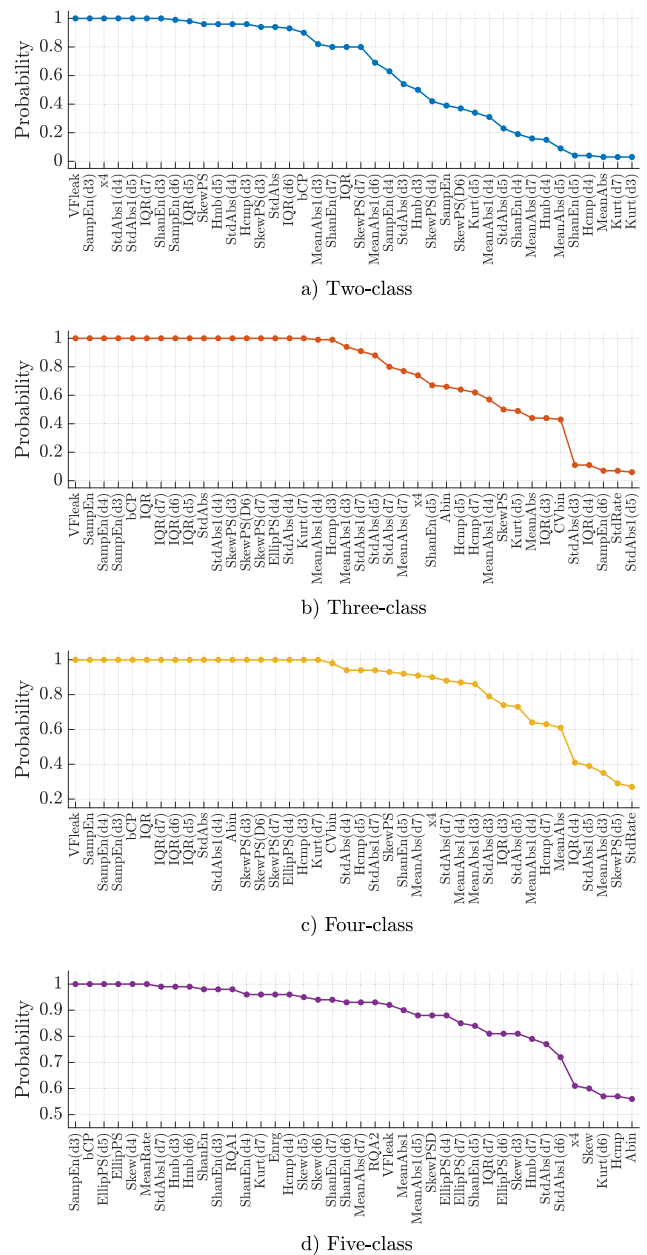

FIGURE 6. Selection probability for the 40 most selected features in the 500 runs of feature selection (outer loop).

80 (30.0-150.0) and 125 (50.0-200.0) for the cases of 4 and 5-classes.

Fig. 4 also shows that the sensitivity for the classes with lower prevalence (VT and PR) increases with shallower trees. In the 4-class classifier the sensitivity for VT increased by more than 40 points when l_{size} was raised from 1 to 100, while the sensitivities of the most prevalent classes (AS, ORG, and VF) decreased very slightly. A similar behavior was observed for the sensitivities of VT and PR in the 5-class problem, although in this case the sensitivity of PEA, the rhythm that borders PR and VT, decreased considerably from 83.1% to 25.1%. PEA sensitivity could be better addressed using
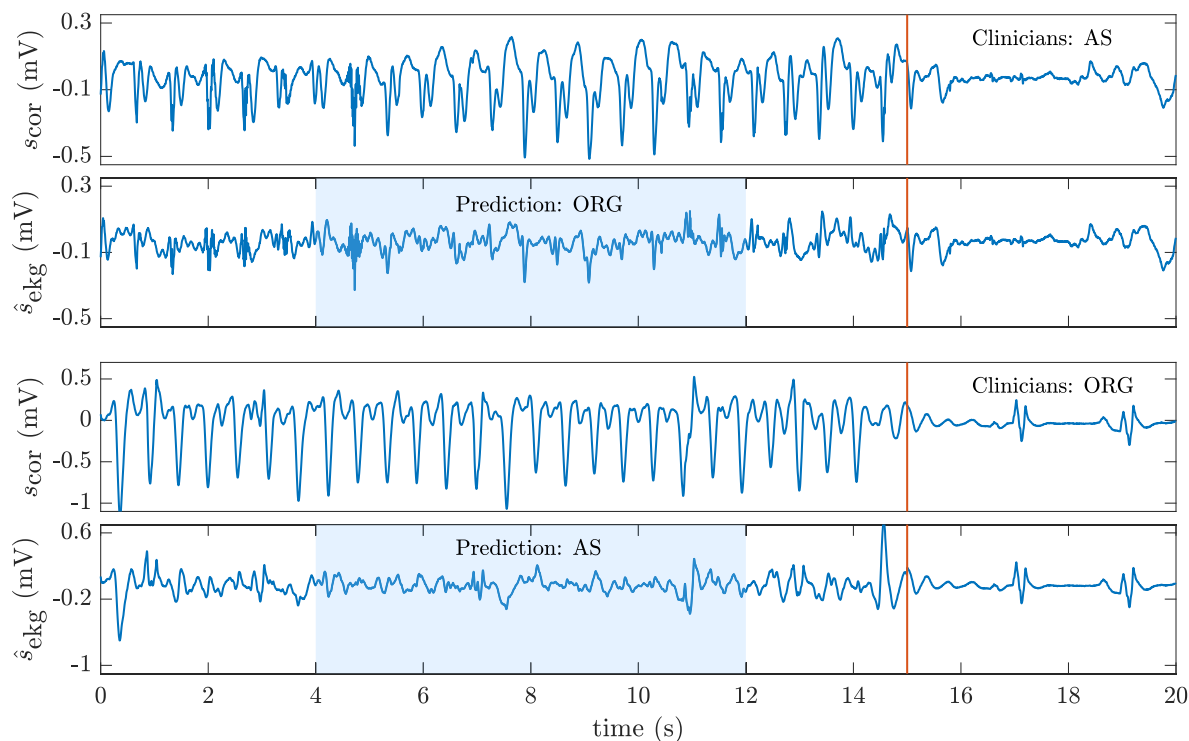
FIGURE 7. Two examples of misclassified segments for the 3-class classifier. In the top panel an AS is classified as ORG, while the bottom panel shows an ORG misclassified as AS.

multimodal analysis by adding information on perfusion from other signals like pulse oximetry, invasive blood pressure, brain oximetry or expired CO_2 when available [54], [55].

Changing the number of trees, B, and the features per split, m_{try}, had less impact on classification. Fig. 5 shows the median UMS of the 50 random repetitions of the 5-class classifier for different choices of B and m_{try}, with $l_{size} = 125$. The figure shows that our preliminary design choices were sound, the UMS stabilizes for $B > 250$ and the effect of m_{try} on the classification results was small with the median UMS varying between 70.9 % and 72.6 %. So the default $m_{try} = \sqrt{K}$ value was a very acceptable choice.

B. FEATURE SELECTION AND RELEVANCE

Feature design is key in classical machine learning. In our approach, we introduced the SWT for multi-resolution analysis because it allows a better amplitude and statistical characterization of the features than the classical DWT used by Rad *et al.* [15]. In addition soft denoising produced a reconstructed signal from which many classical OHCA rhythm classification features could be better estimated. Fig. 6 shows the 40 features with the highest probability of selection (the most important features) for each classification problem. These probabilities were estimated by counting the number of times the features were selected in the 500 runs of feature selection algorithm (50 repeats of 10-fold outer CV). For the 2-class problem the most relevant features

are a mixture of those derived from the detail coefficients and from the denoised signal and correspond to complexity, frequency, time, and statistical domains. For the 3 and 4-class classifiers, features derived from the phase-space reconstruction of the signals were also relevant. Finally, for the most challenging 5-class classifier, the RQA analysis was also needed to improve classification results. Features like VFleak, SampEn (d_3) and IQR (d_7) were selected in all feature selection runs corresponding to the 2, 3 and 4-class classifiers and SampEn (d_3) was also selected in all the runs of the 5-class classifier. These results are consistent with our previous findings on shock/no-shock decisions during mechanical CPR [21]. Although CPR artifacts present very different characteristics during mechanical and manual CPR, features derived from the SWT decomposition of the filtered EKG seem to be very robust and independent of the filtering residuals, thus are able to capture the distinctive characteristics of OHCA rhythms.

VI. DISCUSSION

The relevance of the detailed classification results presented in Table 1 and Fig. 3 is better understood in the context of the clinical importance of each classification problem, and by providing illustrative examples of the classification errors that show the limitations of our approach. For the Sh/NSh 2-class problem, the median UMS was 95.4%, with median sensitivity for the shockable and nonshockable rhythms of 93.5 % and 97.2 %, respectively. This is a very important problem
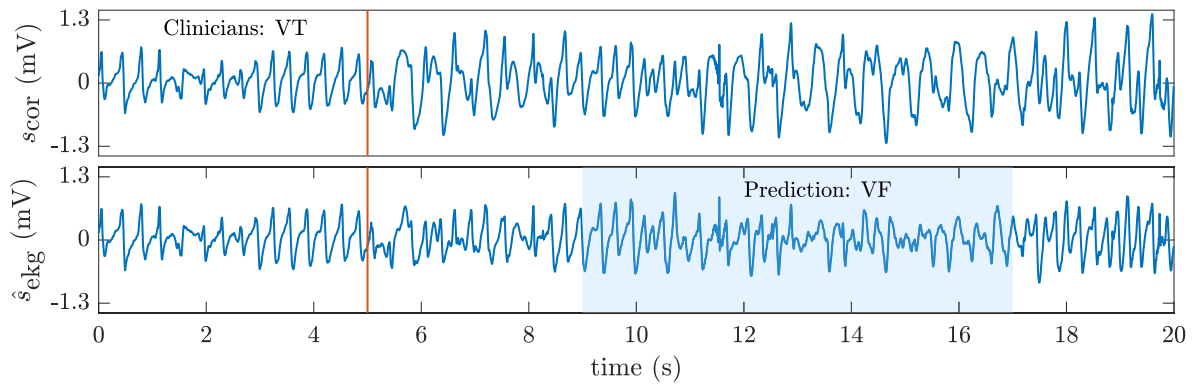
FIGURE 8. An example of a VT classified as VF by the 4-class classifier.
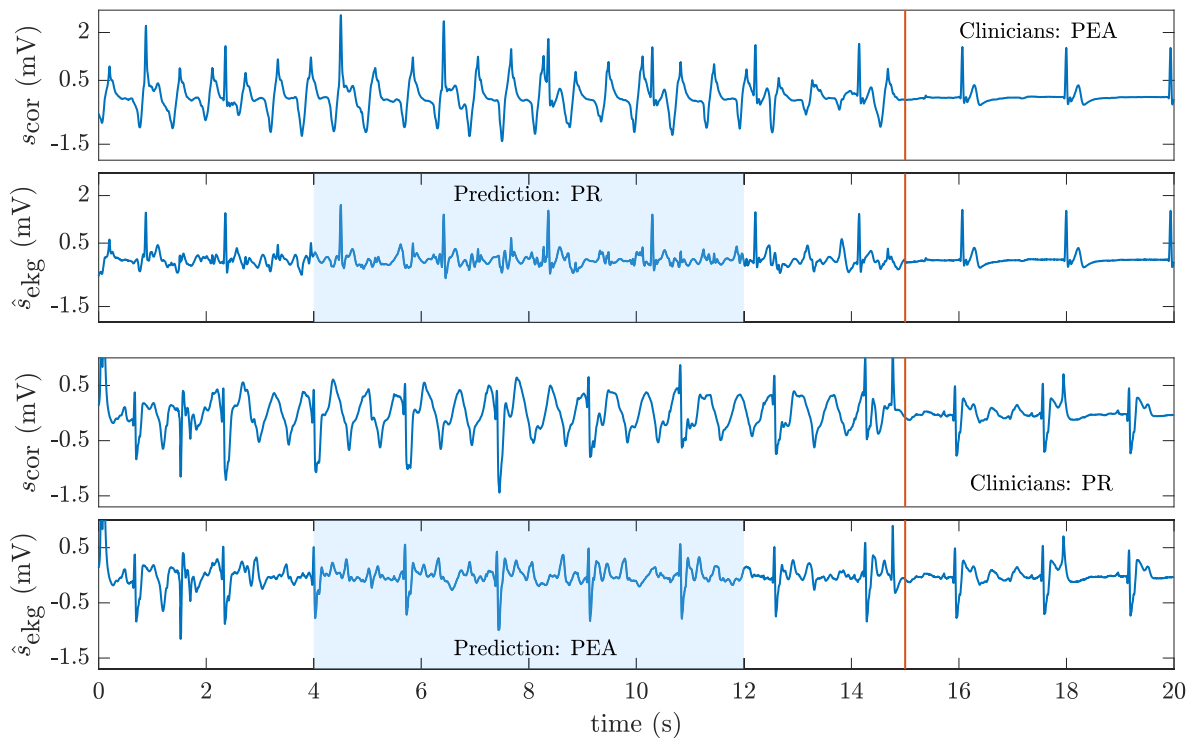

FIGURE 9. Two examples of misclassified PEA/PR rhythms. The last five seconds (clean intervals) of both panels show the difficulty of pulse assessment based only on the EKG.

since it addresses shock advice decisions during CPR. Shock advice algorithms for defibrillators are normally tested on artifact-free data. In that scenario, the American Heart Association requires a minimum sensitivity for shockable and nonshockable rhythms of 90 % and 95 %, respectively [56]. Our solution is above those requirements. Moreover, our results improve by over 1.5-points the UMS reported for the most accurate shock/no-shock algorithms during manual chest compressions [33], [57].

A finer classification of NSh rhythms includes the distinction between AS and ORG rhythms, which can be important to determine pharmacological treatment, or the effect of adrenaline use and dosage during CPR [58]. The UMS for the 3-class classifier was above 87.5 %, and shockable

rhythms had a sensitivity of 93.9%. However, the distinction between AS/ORG during CPR was difficult, 13% of AS were incorrectly classified as ORG whereas a 10.8% of ORG rhythms were classified as AS. These finding are in line with those reported by Kwok *et al.*, who on a limited set of patients demonstrated the first 3-class rhythm classification algorithm during CPR [20]. In scenarios without CPR artifact the distinction between AS/ORG is simple and can be addressed using energy and heart-rate measures [33]. During chest compressions spiky filtering residuals may be confounded as QRS complexes during AS (Fig. 7, top panel). Conversely, CPR artifact filtering may reduce R-peak amplitudes in ORG rhythms producing erroneous AS classifications (Fig. 7, bottom panel).

Classifying shockable rhythms into VT or VF may allow synchronized electrical cardioversion on VT, to avoid the R on T phenomenon that may induce VF. However, the sensitivity for VT dropped considerably in the 4-class problem, 19.7% of VT was classified as VF and 6.3% as ORG. VT rhythms can be confounded as ORG (narrower monomorphic VT) or VF (more irregular Torsades de Pointes). CPR artifacts further complicate the problem since filtering residuals may resemble an irregular VF during VT (see Fig. 8). In any case, the median UMS for the 4-class problem was 80.6%, more than 55-points higher than the 25% value expected for a random guess.

In the 5-class problem, most of the errors were caused by the PEA/PR distinction (presence of pulse in ORG rhythms). Pulse assessment using only the EKG is hard, and determination of pulse during OHCA frequently relies on additional surrogate variables of perfusion like pulse oximetry signals, invasive blood pressure measurements, or expired CO_2 [55], [59]. Fig. 9 shows two representative examples of the difficulty of determining pulse using only the EKG. However, our 5-class classifier had a median UMS of 71.9% during CPR, which is only 5.8-points lower than the 5-class OHCA rhythm classifier on artifact-free EKG proposed by Rad *et al.* [15]. Furthermore, when Rad *et al.*used their algorithms to annotate complete OHCA episodes (no data pruning), the UMS during artifact-free segments was 75%, but dropped to 52.5% in intervals during chest compressions, even after filtering the CPR artifact [27]. Our architecture would therefore substantially improve the accuracy of 5-class classifiers during CPR.

VII. CONCLUSIONS

A robust methodology for OHCA rhythm classification during CPR has been presented. The approach consists of an adaptive CPR artifact suppression filter, followed by feature extraction based on the SWT multiresolution analysis of the EKG, the features are finally fed to a random forest to classify the cardiac rhythm. The approach was successfully demonstrated for 2, 3, 4 and 5-class OHCA cardiac rhythm classification, addressing the most important clinical scenarios for rhythm assessment during CPR. Our method improved the state-of-the-art methods in the extensively studied 2-class shock/no-shock decision scenario, meeting the criteria of the American Heart Association for artifact-free EKG. To the best of our knowledge, we introduced the first general framework for multi-class OHCA rhythm classification during CPR with increasing levels of clinical detail, and our approach substantially improved the accuracy of 5-class OHCA cardiac rhythm classifiers during CPR.

REFERENCES

[1] J.-T. Gräsner *et al.*, "EuReCa ONE-27 nations, ONE Europe, ONE registry: A prospective one month analysis of out-of-hospital cardiac arrest outcomes in 27 countries in Europe," *Resuscitation*, vol. 105, pp. 188–195, Aug. 2016.

[2] G. D. Perkins, A. J. Handley, R. W. Koster, M. Castrén, M. A. Smyth, T. Olasveengen, K. G. Monsieurs, V. Raffay, J.-T. Gräsner, V. Wenzel, G. Ristagno, and J. Soar, "European resuscitation council guidelines for resuscitation 2015: Section 2. Adult basic life support and automated external defibrillation," *Resuscitation*, vol. 95, pp. 81–99, Oct. 2015.

[3] T. Nordseth, D. E. Niles, T. Eftestøl, R. M. Sutton, U. Irusta, B. S. Abella, R. A. Berg, V. M. Nadkarni, and E. Skogvoll, "Rhythm characteristics and patterns of change during cardiopulmonary resuscitation for in-hospital paediatric cardiac arrest," *Resuscitation*, vol. 135, pp. 45–50, Feb. 2019.

[4] T. Nordseth, D. Bergum, D. P. Edelson, T. M. Olasveengen, T. Eftestøl, R. Wiseth, B. S. Abella, and E. Skogvoll, "Clinical state transitions during advanced life support (ALS) in in-hospital cardiac arrest," *Resuscitation*, vol. 84, no. 9, pp. 1238–1244, 2013.

[5] J. T. Kvaløy, E. Skogvoll, T. Eftestøl, K. Gundersen, J. Kramer-Johansen, T. M. Olasveengen, and P. A. Steen, "Which factors influence spontaneous state transitions during resuscitation?" *Resuscitation*, vol. 80, no. 8, pp. 863–869, 2009.

[6] E. Skogvoll, T. Eftestøl, K. Gundersen, J. T. Kvaløy, J. Kramer-Johansen, T. M. Olasveengen, and P. A. Steen, "Dynamics and state transitions during resuscitation in out-of-hospital cardiac arrest," *Resuscitation*, vol. 78, no. 1, pp. 30–37, 2008.

[7] A. B. Rad, K. Engan, A. K. Katsaggelos, J. T. Kvaløy, L. Wik, U. Irusta, and T. Eftestøl, "Automatic cardiac rhythm interpretation during resuscitation," *Resuscitation*, vol. 102, pp. 44–50, May 2016.

[8] E. Alonso, E. Aramendi, M. Daya, U. Irusta, B. Chicote, J. K. Russell, and L. G. Tereshchenko, "Circulation detection using the electrocardiogram and the thoracic impedance acquired by defibrillation pads," *Resuscitation*, vol. 99, pp. 56–62, Feb. 2016.

[9] U. Irusta, J. Ruiz, E. Aramendi, S. R. de Gauna, U. Ayala, and E. Alonso, "A high-temporal resolution algorithm to discriminate shockable from nonshockable rhythms in adults and children," *Resuscitation*, vol. 83, no. 9, pp. 1090–1097, 2012.

[10] Q. Li, C. Rajagopalan, and G. D. Clifford, "Ventricular fibrillation and tachycardia classification using a machine learning approach," vol. 61, no. 3, pp. 1607–1613, Jun. 2013.

[11] C. Figuera, U. Irusta, E. Morgado, E. Aramendi, U. Ayala, L. Wik, J. Kramer-Johansen, T. Eftestøl, and F. Alonso-Atienza, "Machine learning techniques for the detection of shockable rhythms in automated external defibrillators," *PLoS ONE*, vol. 11, no. 7, 2016, Art. no. e0159654.

[12] M. S. Link, L. C. Berkow, P. J. Kudenchuk, H. R. Halperin, E. P. Hess, V. K. Moitra, R. W. Neumar, B. J. O'Neil, J. H. Paxton, S. M. Silvers, R. D. White, D. Yannopoulos, and M. W. Donnino, "Part 7: Adult advanced cardiovascular life support: 2015 American heart association guidelines update for cardiopulmonary resuscitation and emergency cardiovascular care," *Circulation*, vol. 132, pp. S444–S464, Nov. 2015.

[13] M. Risdal, S. O. Aase, J. Kramer-Johansen, and T. Eftesol, "Automatic identification of return of spontaneous circulation during cardiopulmonary resuscitation," *IEEE Trans. Biomed. Eng.*, vol. 55, no. 1, pp. 60–68, Jan. 2008.

[14] A. Elola, E. Aramendi, U. Irusta, J. D. Ser, E. Alonso, and M. Daya, "ECG-based pulse detection during cardiac arrest using random forest classifier," *Med. Biol. Eng. Comput.*, vol. 57, no. 2, pp. 453–462, 2019.

[15] A. B. Rad, T. Eftestøl, K. Engan, U. Irusta, J. T. Kvaløy, J. Kramer-Johansen, L. Wik, and A. K. Katsaggelos, "ECG-based classification of resuscitation cardiac rhythms for retrospective data analysis," *IEEE Trans. Biomed. Eng.*, vol. 64, no. 10, pp. 2411–2418, Oct. 2017.

[16] I. Jekova and V. Krasteva, "Real time detection of ventricular fibrillation and tachycardia," *Physiol. Meas.*, vol. 25, no. 5, p. 1167, 2004.

[17] N. V. Thakor, Y.-S. Zhu, and K.-Y. Pan, "Ventricular tachycardia and fibrillation detection by a sequential hypothesis testing algorithm," *IEEE Trans. Biomed. Eng.*, vol. 37, no. 9, pp. 837–843, Sep. 1990.

[18] U. Irusta and J. Ruiz, "An algorithm to discriminate supraventricular from ventricular tachycardia in automated external defibrillators valid for adult and paediatric patients," *Resuscitation*, vol. 80, no. 11, pp. 1229–1233, 2009.

[19] A. Neurauter, T. Eftestøl, J. Kramer-Johansen, B. S. Abella, K. Sunde, V. Wenzel, K. H. Lindner, J. Eilevstjønn, H. Myklebust, P. A. Steen, and H.-U. Strohmenger, "Prediction of countershock success using single features from multiple ventricular fibrillation frequency bands and feature combinations using neural networks," *Resuscitation*, vol. 73, no. 2, pp. 253–263, 2007.

[20] H. Kwok, J. Coult, M. Drton, T. D. Rea, and L. Sherman, "Adaptive rhythm sequencing: A method for dynamic rhythm classification during CPR," *Resuscitation*, vol. 91, pp. 26–31, Jun. 2015.

[21] I. Isasi, U. Irusta, A. Elola, E. Aramendi, U. Ayala, E. Alonso, J. Kramer-Johansen, and T. Eftestøl, "A machine learning shock decision algorithm for use during piston-driven chest compressions," *IEEE Trans. Biomed. Eng.*, vol. 66, no. 6, pp. 1752–1760, Jun. 2019.

[22] B. Chicote, U. Irusta, R. Alcaraz, J. J. Rieta, E. Aramendi, I. Isasi, D. Alonso, and K. Ibarguren, "Application of entropy-based features to predict defibrillation outcome in cardiac arrest," *Entropy*, vol. 18, no. 9, p. 313, 2016.

[23] B. Chicote, U. Irusta, E. Aramendi, R. Alcaraz, J. J. Rieta, I. Isasi, D. Alonso, M. D. M. Baqueriza, and K. Ibarguren, "Fuzzy and sample entropies as predictors of patient survival using short ventricular fibrillation recordings during out of hospital cardiac arrest," *Entropy*, vol. 20, no. 8, p. 591, 2018.

[24] D. Cabello, S. Barro, J. M. Salceda, R. Ruiz, and J. Mira, "Fuzzy K-nearest neighbor classifiers for ventricular arrhythmia detection," *Int. J. Bio-Med. Comput.*, vol. 27, no. 2, pp. 77–93, 1991.

[25] Y. Alwan, Z. Cvetković, and M. J. Curtis, "Methods for improved discrimination between ventricular fibrillation and tachycardia," *IEEE Trans. Biomed. Eng.*, vol. 65, no. 10, pp. 2143–2151, Oct. 2018.

[26] P. Cheng and X. Dong, "Life-threatening ventricular arrhythmia detection with personalized features," *IEEE Access*, vol. 5, pp. 14195–14203, 2017.

[27] A. B. Rad, T. Eftestøl, U. Irusta, J. T. Kvaløy, L. Wik, J. Kramer-Johansen, A. K. Katsaggelos, and K. Engan, "An automatic system for the comprehensive retrospective analysis of cardiac rhythms in resuscitation episodes," *Resuscitation*, vol. 122, pp. 6–12, Jan. 2018.

[28] S. Cheskes, R. H. Schmicker, J. Christenson, D. D. Salcido, T. Rea, J. Powell, D. P. Edelson, R. Sell, S. May, J. J. Menegazzi, L. Van Ottingham, M. Olsufka, S. Pennington, J. Simonini, R. A. Berg, I. Stiell, A. Idris, B. Bigham, L. Morrison, and R. O. C. R. Investigators, "Perishock pause: An independent predictor of survival from out-of-hospital shockable cardiac arrest," *Circulation*, vol. 124, pp. 58–66, Jul. 2011.

[29] S. R. de Gauna, U. Irusta, J. Ruiz, U. Ayala, E. Aramendi, and T. Eftestøl, "Rhythm analysis during cardiopulmonary resuscitation: Past, present, and future," *BioMed Res. Int.*, vol. 2014, Jan. 2014, Art. no. 386010.

[30] J. Eilevstjønn, T. Eftestøl, S. O. Aase, H. Myklebust, J. H. Husøy, and P. A. Steen, "Feasibility of shock advice analysis during CPR through removal of CPR artefacts from the human ECG," *Resuscitation*, vol. 61, pp. 131–141, May 2004.

[31] U. Irusta, J. Ruiz, S. R. D. Gauna, T. Eftestøl, and J. Kramer-Johansen, "A least mean-square filter for the estimation of the cardiopulmonary resuscitation artifact based on the frequency of the compressions," *IEEE Trans. Biomed. Eng.*, vol. 56, no. 4, pp. 1052–1062, Apr. 2009.

[32] I. Isasi, U. Irusta, E. Aramendi, U. Ayala, E. Alonso, J. Kramer-Johansen, and T. Eftestøl, "A multistage algorithm for ECG Rhythm analysis during piston-driven mechanical chest compressions," *IEEE Trans. Biomed. Eng.*, vol. 66, no. 1, pp. 263–272, Jan. 2019.

[33] U. Ayala, U. Irusta, J. Ruiz, T. Eftestøl, J. Kramer-Johansen, F. Alonso-Atienza, E. Alonso, and D. González-Otero, "A reliable method for rhythm analysis during cardiopulmonary resuscitation," *BioMed Res. Int.*, vol. 2014, Mar. 2014, Art. no. 872470.

[34] L. Wik, J. Kramer-Johansen, H. Myklebust, H. Sørebø, L. Svensson, B. Fellows, and P. A. Steen, "Quality of cardiopulmonary resuscitation during out-of-hospital cardiac arrest," *JAMA*, vol. 293, no. 3, pp. 299–304, 2005.

[35] J. Kramer-Johansen, H. Myklebust, L. Wik, B. Fellows, L. Svensson, H. Sørebø, and P. A. Steen, "Quality of out-of-hospital cardiopulmonary resuscitation with real time automated feedback: A prospective interventional study," *Resuscitation*, vol. 71, no. 3, pp. 283–292, 2006.

[36] S. O. Aase and H. Myklebust, "Compression depth estimation for CPR quality assessment using DSP on accelerometer signals," *IEEE Trans. Biomed. Eng.*, vol. 49, no. 3, pp. 263–268, Mar. 2002.

[37] Y. Xiao, L. Ma, and R. K. Ward, "Fast RLS Fourier analyzers capable of accommodating frequency mismatch," *Signal Process.*, vol. 87, no. 9, pp. 2197–2212, 2007.

[38] J. E. Fowler, "The redundant discrete wavelet transform and additive noise," *IEEE Signal Process. Lett.*, vol. 12, no. 9, pp. 629–632, Sep. 2005.

[39] D. L. Donoho and J. M. Johnstone, "Ideal spatial adaptation by wavelet shrinkage," *Biometrika*, vol. 81, no. 3, pp. 425–455, 1994.

[40] P. S. Hamilton and W. J. Tompkins, "Quantitative investigation of QRS detection rules using the MIT/BIH arrhythmia database," *IEEE Trans. Biomed. Eng.*, vol. BME-33, no. 12, pp. 1157–1165, Dec. 1986.

[41] S. Kuo, "Computer detection of ventricular fibrillation," in *Proc. IEEE Comput. Soc. Comput. Cardiol.*, 1978, pp. 347–349.

[42] I. Jekova, "Shock advisory tool: Detection of life-threatening cardiac arrhythmias and shock success prediction by means of a common parameter set," *Biomed. Signal Process. Control*, vol. 2, no. 1, pp. 25–33, 2007.

[43] F. Alonso-Atienza, E. Morgado, L. Fernández-Martínez, A. García-Alberola, and J. L. Rojo-Álvarez, "Detection of life-threatening arrhythmias using feature selection and support vector machines," *IEEE Trans. Biomed. Eng.*, vol. 61, no. 3, pp. 832–840, Mar. 2014.

[44] L. Gonzalez, K. Walker, S. Challa, and B. Bent, "Monitoring a skipped heartbeat: A real-time premature ventricular contraction (PVC) monitor," in *Proc. IEEE Virtual Conf. Appl. Commercial Sensors (VCACS)*, Jun./Jul. 2017, pp. 1–7.

[45] F. Takens, "Detecting strange attractors in turbulence," in *Dynamical Systems and Turbulence, Warwick* (Lecture Notes in Mathematics), vol. 898. Springer, Oct. 2006, pp. 366–381.

[46] M. Zabihi, A. B. Rad, A. K. Katsaggelos, S. Kiranyaz, S. Narkilahti, and M. Gabbouj, "Detection of atrial fibrillation in ECG hand-held devices using a random forest classifier," in *Proc. Comput. Cardiol. (CinC)*, Sep. 2017, pp. 1–4.

[47] N. Marwan, N. Wessel, U. Meyerfeldt, A. Schirdewan, and J. Kurths, "Recurrence-plot-based measures of complexity and their application to heart-rate-variability data," *Phys. Rev. E, Stat. Phys. Plasmas Fluids Relat. Interdiscip. Top.*, vol. 66, no. 2, 2002, Art. no. 026702.

[48] D. Krstajic, L. J. Buturovic, D. E. Leahy, and S. Thomas, "Cross-validation pitfalls when selecting and assessing regression and classification models," *J. Cheminform.*, vol. 6, no. 1, p. 10, Mar. 2014.

[49] B. Gregorutti, B. Michel, and P. Saint-Pierre, "Correlation and variable importance in random forests," *Statist. Comput.*, vol. 27, no. 3, pp. 659–678, 2017.

[50] L. Breiman, "Random forests," *Mach. Learn.*, vol. 45, no. 1, pp. 5–32, 2001.

[51] R. Díaz-Uriarte and S. A. De Andrés, "Gene selection and classification of microarray data using random forest," *BMC Bioinf.*, vol. 7, no. 1, p. 3, 2006.

[52] H. Pang, S. L. George, K. Hui, and T. Tong, "Gene selection using iterative feature elimination random forests for survival outcomes," *IEEE/ACM Trans. Comput. Biol. Bioinf.*, vol. 9, no. 5, pp. 1422–1431, Sep. 2012.

[53] K. Q. Shen, C. J. Ong, X. P. Li, Z. Hui, and E. P. V. Wilder-Smith, "A feature selection method for multilevel mental fatigue EEG classification," *IEEE Trans. Biomed. Eng.*, vol. 54, no. 7, pp. 1231–1237, Jul. 2007.

[54] P. Hubner, R. W. C. G. R. Wijshoff, J. Muehlsteff, C. Wallmüller, A. M. Warenits, I. A. M. Magnet, K. Nammi, J. K. Russell, and F. Sterz, "A series of case studies on detection of spontaneous pulse by photo-plethysmography in cardiopulmonary resuscitation," *Amer. J. Emergency Med.*, to be published.

[55] A. Elola, E. Aramendi, U. Irusta, E. Alonso, Y. Lu, M. P. Chang, P. Owens, and A. H. Idris, "Capnography: A support tool for the detection of return of spontaneous circulation in out-of-hospital cardiac arrest," *Resuscitation*, to be published.

[56] R. E. Kerber, L. B. Becker, J. D. Bourland, R O. Cummins, A. P. Hallstrom, M. B. Michos, G. Nichol, J. P. Ornato, W. H. Thies, R. D. White, and B. D. Zuckerman, "Automatic external defibrillators for public access defibrillation: Recommendations for specifying and reporting arrhythmia analysis algorithm performance, incorporating new waveforms, and enhancing safety: A statement for health professionals from the American heart association task force on automatic external defibrillation, subcommittee on aed safety and efficacy," *Circulation*, vol. 95, no. 6, pp. 1677–1682, 1997.

[57] V. Krasteva, I. Jekova, I. Dotsinsky, and J.-P. Didon, "Shock advisory system for heart rhythm analysis during cardiopulmonary resuscitation using a single ECG input of automated external defibrillators," *Ann. Biomed. Eng.*, vol. 38, no. 4, pp. 1326–1336, 2010.

[58] R. R. Attaran and G. A. Ewy, "Epinephrine in resuscitation: Curse or cure?" *Future Cardiol.*, vol. 6, no. 4, pp. 473–482, 2010.

[59] R. W. C. G. R. Wijshoff, A. M. T. M. van Asten, W. H. Peeters, R. Bezemer, G. J. Noordergraaf, M. Mischi, and R. M. Aarts, "Photoplethysmography-based algorithm for detection of cardiogenic output during cardiopulmonary resuscitation," *IEEE Trans. Biomed. Eng.*, vol. 62, no. 3, pp. 909–921, Mar. 2015.

IRAIA ISASI was born in Bilbao in 1992. She received the B.Sc. and M.Sc. degrees in telecommunications engineering from the University of the Basque Country, in 2014 and 2016, respectively, where she is currently pursuing the Ph.D. degree. Her research is focused on applications of biomedical signal processing and machine learning techniques applied to improve therapy during cardiac arrest. She has made contributions to automatic ECG rhythm analysis during cardiopulmonary resuscitation.

MORTEZA ZABIHI was born in Mashhad, Iran, in 1988. He received the M.Sc. degree in biomedical engineering from Tampere University, Tampere, Finland, in 2013. He is currently pursuing the Ph.D. degree with the Department of Computing Sciences, Tampere University, Tampere, Finland, where he is a Researcher. His research interests include nonlinear dynamics and time series analysis, pattern recognition, and machine learning with application to EEG and ECG signal processing. Since 2015, he has been ranked in the top three teams in series of international competitions such as PhysioNet/Computing in Cardiology Challenges. He has accomplished five conferences and three peer-reviewed major journal articles from his Ph.D. theses work.

UNAI IRUSTA was born in Bilbao in 1973. He received the M.Sc. degree (Hons.) in telecommunications engineering from the University of the Basque Country, in 1998, where he has been an Assistant Professor, since 2003 and an Associate Professor, since 2011. His field of expertise is biomedical signal processing, machine learning, and data management in the field of prehospital emergency medicine and cardiac arrest. In the above field, he has published 39 papers in SCI-IF journals and over 90 contributions to scientific conferences.

TRYGVE EFTESTØL was born in Bergen, Norway, in 1967. He received the B.Eng. degree in electrical engineering from the Bergen College, Bergen, in 1992, the M.Sc. degree in cybernetics, and the Ph.D. degree in signal processing from the Stavanger University College, Stavanger, Norway, in 1994 and 2000, respectively. He is currently a Professor with the Department of Electrical and Computer Engineering, University of Stavanger, where he is also with the Biomedical Data Analysis Laboratory. His main research interests include biomedical signal and image analysis, and pattern recognition. In this field, he has published 75 papers in SCI-IF journals and over 100 contributions to scientific conferences.

ALI BAHRAMI RAD received the B.Sc. degree in electrical engineering from Imam Hossein University, Tehran, Iran, in 2003, the M.Sc. degree in biomedical engineering from the Tampere University of Technology, Tampere, Finland, in 2011, and the Ph.D. degree in computer engineering—information technology from the University of Stavanger, Stavanger, Norway, in 2017. He is currently a Postdoctoral Researcher with the Electrical Engineering and Automation Department, Aalto University, Espoo, Finland. His current research interests include machine learning, neural systems, and biosignal analysis. He was a recipient of several international prizes in biosignal analysis and machine learning contests, including PhysioNet/Computing in Cardiology Challenge 2017 (tied for the 1st place), PhysioNet/Computing in Cardiology Challenge 2016 (second place), and Brain–Computer Interface Challenge at IEEE EMBS Neural Engineering Conference 2015 (third place).

JO KRAMER-JOHANSEN was born in Norway in 1969. He received the M.D. degree from the University of Oslo, Oslo, Norway, in 1995, and qualified as a Specialist in anesthesiology and intensive care, in 2003, and the Ph.D. degree from the University of Oslo, in 2007. He is currently an Anesthesiologist with the Division of Prehospital Services, Oslo University Hospital and a Professor at the University of Oslo. He is also a Scientific Head of the Norwegian Cardiac Arrest Registry and leads the Prehospital Research Group at the University of Oslo. His research interests include cardiac arrest epidemiology, training and treatment, and more general implementation of science into clinical practice. In the above field, he has published 75 papers in SCI-IF journals and more than 100 contributions to scientific conferences.

ELISABETE ARAMENDI received the Ph.D. degree in telecommunications engineering. She joined the Telecommunication Engineering Department of the University of the Basque Country, in 1994, where she has been an Associate Professor, since 2002, teaching advanced statistical signal processing. Her research is centered in the application of signal processing techniques in bioengineering, focused on topics related to resuscitation and treatment of cardiac arrest. In the above field, she has published 32 papers in SCI-IF and more than 90 contributions to scientific conferences.

LARS WIK was born in Oslo, Norway, in 1957. He received the cand med degree from the University of Oslo, Oslo, Norway, in 1986 and qualified as a Specialist in anesthesiology, in 2011, and the Ph.D. degree from the University of Oslo, in 1996. He is currently a Consultant in anesthesiology and a Senior Researcher with the Oslo University Hospital, Oslo, Norway. His current research interests include quality and outcome of cardiopulmonary resuscitation and traffic accident research with trauma. In these fields, he has published over 90 papers in SCI-IF journals and over 100 contributions to scientific conferences.

● ● ●